A one-field discontinuous Galerkin formulation of non-linear Kirchhoff-Love shells

Ludovic Noels

Computational & Multiscale Mechanics of Materials, ULg
Chemin des Chevreuils 1, B4000 Liège, Belgium
L.Noels@ulg.ac.be

Discontinuous Galerkin Methods

- Main idea
  - Finite-element discretization
  - Same **discontinuous** polynomial approximations for the
    - **Test** functions φ_h and
    - **Trial** functions $\delta\varphi$

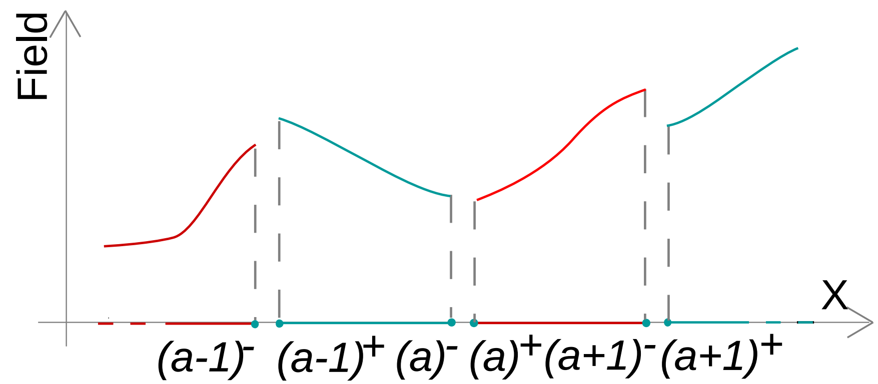

  - Definition of operators on the interface trace:
    - **Jump** operator: $[\![\bullet]\!] = \bullet^+ - \bullet^-$
    - **Mean** operator: $\langle\bullet\rangle = \frac{\bullet^+ + \bullet^-}{2}$
  - Continuity is weakly enforced, such that the method
    - Is consistent
    - Is stable
    - Has the optimal convergence rate

Discontinuous Galerkin Methods

- Discontinuous Galerkin methods vs Continuous
  - More expensive (more degrees of freedom)
  - More difficult to implement
  - …
- So why discontinuous Galerkin methods?
  - Weak enforcement of C^1 continuity for high-order equations
    - Strain-gradient effect
    - Shells with complex material behaviors
    - Toward computational homogenization of thin structures?
  - Exploitation of the discontinuous mesh to simulate dynamic fracture [Seagraves, Jérusalem, Noels, Radovitzky, col. ULg-MIT]:
    - Correct wave propagation before fracture
    - Easy to parallelize & scalable

Discontinuous Galerkin Methods

- Continuous field / discontinuous derivative
  - No new nodes
  - Weak enforcement of C^1 continuity
  - Displacement formulations of high-order differential equations
  - Usual shape functions in 3D (no new requirement)
  - Applications to
    - Beams, plates [Engel et al., CMAME 2002; Hansbo & Larson, CALCOLO 2002; Wells & Dung, CMAME 2007]
    - Linear & non-linear shells [Noels & Radovitzky, CMAME 2008; Noels IJNME 2009]
    - Damage & Strain Gradient [Wells et al., CMAME 2004; Molari, CMAME 2006; Bala-Chandran et al. 2008]

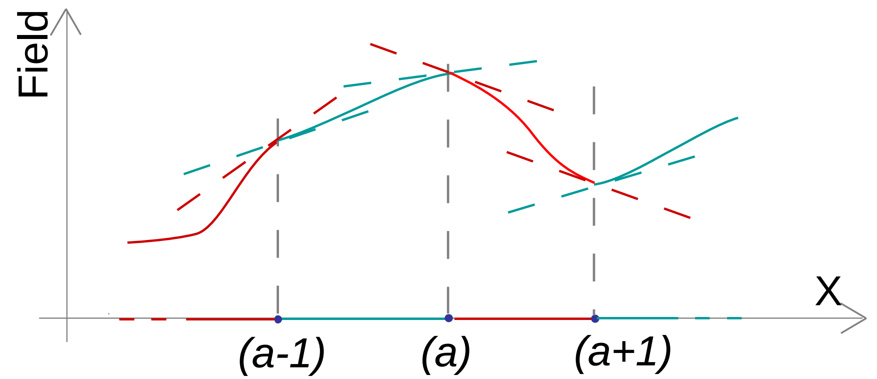

Topics

- Key principles of DG methods
  - Illustration on volume FE
- Kirchhoff-Love Shell Kinematics
- Non-Linear Shells
- Numerical examples
- Conclusions & Perspectives

Key principles of DG methods

- Application to non-linear mechanics
  - Formulation in terms of the first Piola stress tensor **P**

$$\nabla_0 \cdot \mathbf{P}^T = 0 \text{ in } \Omega \quad \& \quad \begin{cases} \mathbf{P} \cdot \boldsymbol{N} = \bar{\boldsymbol{T}} \text{ on } \partial_N \Omega \\ \varphi_h = \bar{\varphi}_h \text{ on } \partial_D B \end{cases}$$

  - New weak formulation obtained by integration by parts **on each element** Ω^e

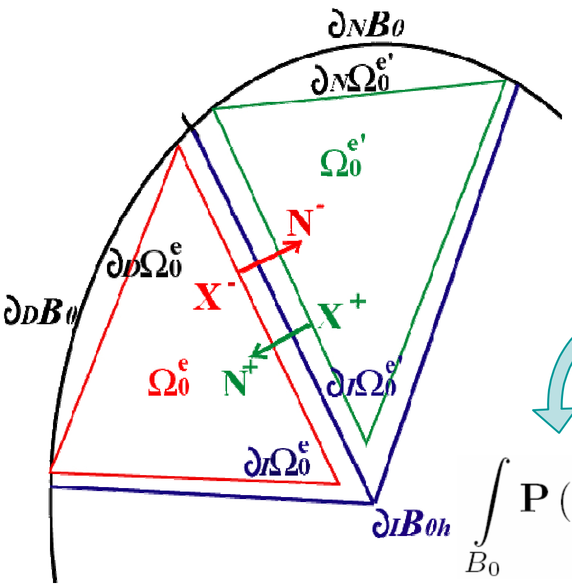

$$\sum_e \int_{\Omega_0^e} \nabla_0 \cdot \mathbf{P}^T(\varphi_h) \cdot \delta\varphi \, dB = 0$$

$$\sum_e \int_{\Omega_0^e} -\mathbf{P}(\varphi_h) : \nabla_0 \delta\varphi \, dB + \sum_e \int_{\partial\Omega_0^e} \delta\varphi \cdot \mathbf{P}(\varphi_h) \cdot \boldsymbol{N} \, d\partial B = 0$$

$$\int_{B_0} \mathbf{P}(\varphi_h) : \nabla_0 \delta\varphi \, dB + \int_{\partial_I B_0} [\![\delta\varphi \cdot \mathbf{P}(\varphi_h)]\!] \cdot \boldsymbol{N}^- \, d\partial B = \int_{\partial_N B_0} \bar{\boldsymbol{T}} \cdot \delta\varphi \, d\partial B$$

?

Key principles of DG methods

- Interface term rewritten as the sum of 3 terms
  - Introduction of the numerical flux ***h***

$$\int_{\partial_I B_0} [\![\delta\boldsymbol{\varphi} \cdot \mathbf{P}(\boldsymbol{\varphi}_h)]\!] \cdot \boldsymbol{N}^- \, d\partial B \rightarrow \int_{\partial_I B_0} [\![\delta\boldsymbol{\varphi}]\!] \cdot \boldsymbol{h}\left(\mathbf{P}^+, \mathbf{P}^-, \boldsymbol{N}^-\right) \, d\partial B$$

    - Has to be consistent: $\begin{cases} \boldsymbol{h}\left(\mathbf{P}^+, \mathbf{P}^-, \boldsymbol{N}^-\right) = -\boldsymbol{h}\left(\mathbf{P}^-, \mathbf{P}^+, \boldsymbol{N}^+\right) \\ \boldsymbol{h}\left(\mathbf{P}_{\text{exact}}, \mathbf{P}_{\text{exact}}, \boldsymbol{N}^-\right) = \mathbf{P}_{\text{exact}} \cdot \boldsymbol{N}^- \end{cases}$
    - One possible choice: $\boldsymbol{h}\left(\mathbf{P}^+, \mathbf{P}^-, \boldsymbol{N}^-\right) = \langle \mathbf{P} \rangle \cdot \boldsymbol{N}^-$
  - Weak enforcement of the compatibility

$$\int_{\partial_I B_0} [\![\boldsymbol{\varphi}_h]\!] \cdot \left\langle \frac{\partial \mathbf{P}}{\partial \mathbf{F}} : \boldsymbol{\nabla}_0 \delta\boldsymbol{\varphi} \right\rangle \cdot \boldsymbol{N}^- \, d\partial B$$

  - Stabilization controlled by parameter β, for all mesh sizes h^s

$$\int_{\partial_I B_0} [\![\boldsymbol{\varphi}_h]\!] \otimes \boldsymbol{N}^- : \left\langle \frac{\beta}{h^s} \frac{\partial \mathbf{P}}{\partial \mathbf{F}} \right\rangle : [\![\delta\boldsymbol{\varphi}]\!] \otimes \boldsymbol{N}^- \, d\partial B$$

Noels & Radovitzky, IJNME 2006 & JAM 2006

  - These terms can also be explicitly derived from a variational formulation (Hu-Washizu-de Veubeke functional)

Key principles of DG methods

- Numerical applications
  - Properties for a polynomial approximation of order *k*
    - Consistent, stable for $\beta > C^k$, convergence in the e-norm in *k*
    - Explicit time integration with conditional stability $\Delta t_{\mathrm{crit}} = \frac{h^s}{\sqrt{\beta}}\sqrt{\frac{\rho_0}{E}}$
    - High scalability
  - Examples

Taylor's impact

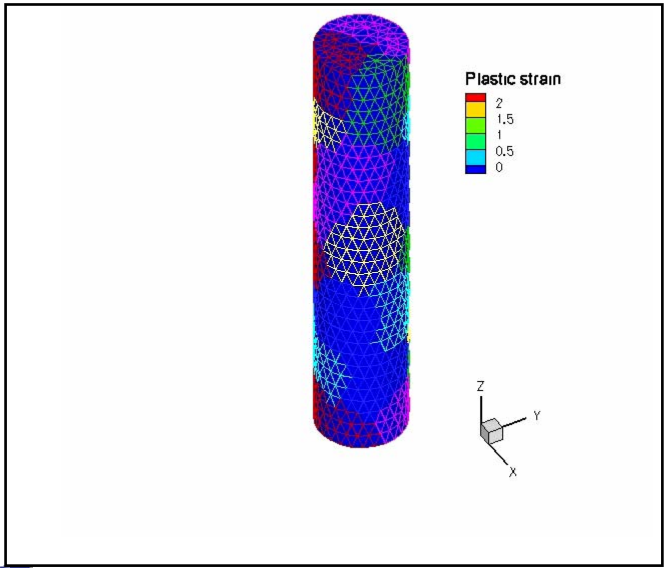

Wave propagation

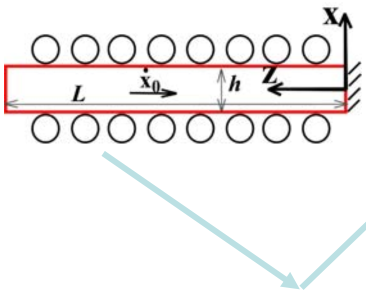

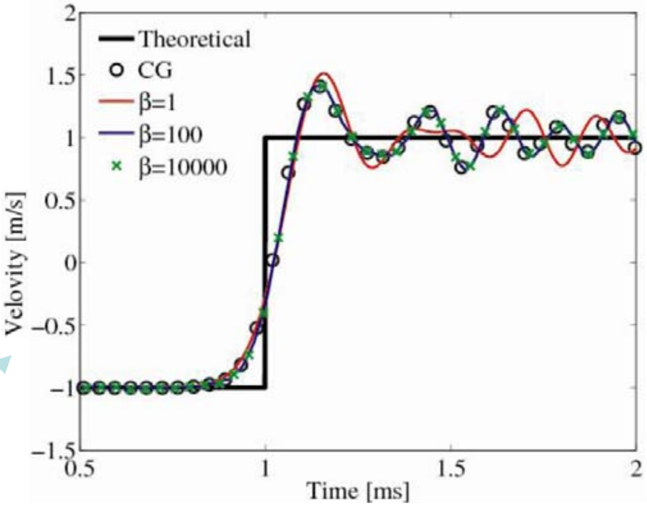

Time evolution of the free face velocity

Kirchhoff-Love Shell Kinematics

- Description of the thin body

$$\boldsymbol{x} = \boldsymbol{\Phi}\left(\xi^I\right) = \boldsymbol{\varphi}\left(\xi^\alpha\right) + \xi^3 \lambda_h \boldsymbol{t}\left(\xi^\alpha\right)$$

Mapping of the mid-surface

Thickness stretch

Mapping of the normal to the mid-surface

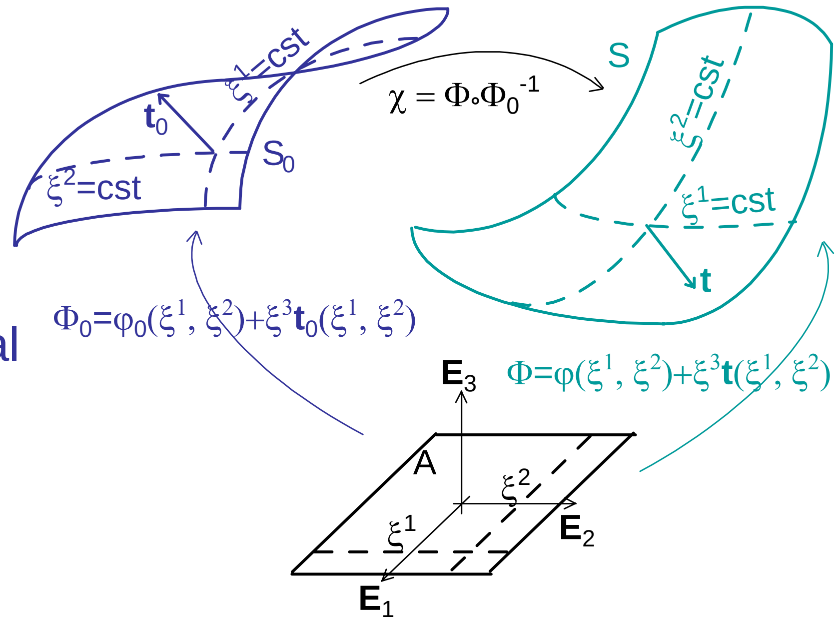

- Deformation mapping

$\mathbf{F} = \boldsymbol{\nabla}\boldsymbol{\Phi} \circ \left[\boldsymbol{\nabla}\boldsymbol{\Phi}_0\right]^{-1}$ with

$\boldsymbol{\nabla}\boldsymbol{\Phi} = \boldsymbol{g}_i \otimes \boldsymbol{E}^i$ & $\boldsymbol{g}_i = \boldsymbol{\nabla}\boldsymbol{\Phi}\boldsymbol{E}_i = \frac{\partial \boldsymbol{\Phi}}{\partial \xi^i}$

$\Longrightarrow$ $\boldsymbol{g}_\alpha = \frac{\partial \boldsymbol{\Phi}}{\partial \xi^\alpha} = \boldsymbol{\varphi}_{,\alpha} + \xi^3 \lambda_h \boldsymbol{t}_{,\alpha} + \xi^3 \boldsymbol{t} \lambda_{h,\alpha}$ & $\boldsymbol{g}_3 = \frac{\partial \boldsymbol{\Phi}}{\partial \xi^3} = \lambda_h \boldsymbol{t}$

- Shearing is neglected

$\Longrightarrow$ $\boldsymbol{t} = \frac{\boldsymbol{\varphi}_{,1} \wedge \boldsymbol{\varphi}_{,2}}{\left\|\boldsymbol{\varphi}_{,1} \wedge \boldsymbol{\varphi}_{,2}\right\|}$ & the gradient of thickness stretch $\lambda_{h,\alpha}$ neglected

Kirchhoff-Love Shell Kinematics

- Resultant equilibrium equations:
  - Linear momentum $\frac{1}{\bar{j}}\left(\bar{j}\boldsymbol{n}^{\alpha}\right)_{,\alpha} + \boldsymbol{n}^{\mathcal{A}} = 0$
  - Angular momentum $\frac{1}{\bar{j}}\left(\bar{j}\tilde{\boldsymbol{m}}^{\alpha}\right)_{,\alpha} - \boldsymbol{l} + \lambda\boldsymbol{t} + \tilde{\boldsymbol{m}}^{\mathcal{A}} = 0$
  - In terms of resultant stresses:

$$\begin{cases} \boldsymbol{n}^{\alpha} = \frac{1}{\bar{j}}\int_{h_{\min 0}}^{h_{\max 0}} \boldsymbol{\sigma}\boldsymbol{g}^{\alpha}\det\left(\boldsymbol{\nabla\Phi}\right) d\xi^{3} \\ \tilde{\boldsymbol{m}}^{\alpha} = \frac{1}{\bar{j}}\int_{h_{\min 0}}^{h_{\max 0}} \xi^{3}\boldsymbol{\sigma}\boldsymbol{g}^{\alpha}\det\left(\boldsymbol{\nabla\Phi}\right) d\xi^{3} \\ \boldsymbol{l} = \frac{1}{\bar{j}}\int_{h_{\min 0}}^{h_{\max 0}} \boldsymbol{\sigma}\boldsymbol{g}^{3}\det\left(\boldsymbol{\nabla\Phi}\right) d\xi^{3} \end{cases}$$

    of resultant applied tension $\boldsymbol{n}^{\mathcal{A}}$ and torque $\tilde{\boldsymbol{m}}^{\mathcal{A}}$

    and of the mid-surface Jacobian $\bar{j} = \|\boldsymbol{\varphi}_{,1} \wedge \boldsymbol{\varphi}_{,2}\|$

Non-linear Shells

- Material behavior
  - Through the thickness integration by Simpson's rule
  - At each Simpson point
    - Internal energy $W(\mathbf{C}=\mathbf{F}^T\mathbf{F})$ with

$$\begin{cases} \mathbf{C} = \boldsymbol{g}_i \cdot \boldsymbol{g}_j \; \boldsymbol{g}_0^i \otimes \boldsymbol{g}_0^j = \mathrm{g}_{ij} \; \boldsymbol{g}_0^i \otimes \boldsymbol{g}_0^j \\ \boldsymbol{\sigma} = \sigma^{ij} \; \boldsymbol{g}_i \otimes \boldsymbol{g}_j = 2 \frac{\det(\boldsymbol{\nabla}\boldsymbol{\Phi}_0)}{\det(\boldsymbol{\nabla}\boldsymbol{\Phi})} \frac{\partial W}{\partial \mathrm{g}_{ij}} \; \boldsymbol{g}_i \otimes \boldsymbol{g}_j \end{cases}$$

    - Iteration on the thickness ratio $\lambda_h = \frac{h_{\max} - h_{\min}}{h_{\max 0} - h_{\min 0}}$ in order to reach the plane stress assumption $\sigma^{33}=0$
  - Simpson's rule leads to the resultant stresses:

$$\begin{cases} \boldsymbol{n}^{\alpha} = \frac{1}{\bar{j}} \int_{h_{\min 0}}^{h_{\max 0}} \boldsymbol{\sigma} \boldsymbol{g}^{\alpha} \det(\boldsymbol{\nabla}\boldsymbol{\Phi}) \, d\xi^3 \\ \tilde{\boldsymbol{m}}^{\alpha} = \frac{1}{\bar{j}} \int_{h_{\min 0}}^{h_{\max 0}} \xi^3 \boldsymbol{\sigma} \boldsymbol{g}^{\alpha} \det(\boldsymbol{\nabla}\boldsymbol{\Phi}) \, d\xi^3 \\ \boldsymbol{l} = \frac{1}{\bar{j}} \int_{h_{\min 0}}^{h_{\max 0}} \boldsymbol{\sigma} \boldsymbol{g}^{3} \det(\boldsymbol{\nabla}\boldsymbol{\Phi}) \, d\xi^3 \end{cases}$$

Non-linear Shells

- Discontinuous Galerkin formulation
  - New weak form obtained from the momentum equations
  - Integration by parts on each element A^e
  - Across 2 elements δt is discontinuous

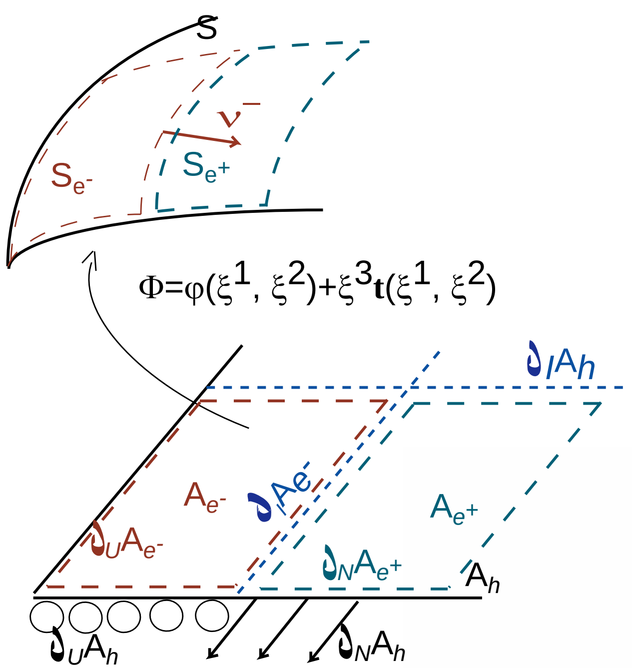

$$0 = \int_{\mathcal{A}_e} \left(\bar{j}\boldsymbol{n}^\alpha(\boldsymbol{\varphi}_h)\right)_{,\alpha} \cdot \delta\boldsymbol{\varphi} d\mathcal{A} + \int_{\mathcal{A}_e} \boldsymbol{n}^\mathcal{A} \cdot \delta\boldsymbol{\varphi}\bar{j} d\mathcal{A} +$$

$$\int_{\mathcal{A}_e} \left[\left(\bar{j}\tilde{\boldsymbol{m}}^\alpha(\boldsymbol{\varphi}_h)\right)_{,\alpha} - \bar{j}\boldsymbol{l}\right] \cdot \delta\boldsymbol{t}\lambda_h d\mathcal{A} + \int_{\mathcal{A}_e} \tilde{\boldsymbol{m}}^\mathcal{A} \cdot \delta\boldsymbol{t}\lambda_h\bar{j} d\mathcal{A}$$

$$-\sum_e \int_{\bar{\mathcal{A}}_e} \bar{j}\tilde{\boldsymbol{m}}^\alpha(\boldsymbol{\varphi}_h) \cdot (\delta\boldsymbol{t}\lambda_h)_{,\alpha} d\mathcal{A} + \sum_e \int_{\partial\mathcal{A}_e} \bar{j}\tilde{\boldsymbol{m}}^\alpha(\boldsymbol{\varphi}_h) \cdot \delta\boldsymbol{t}\lambda_h\nu_\alpha d\mathcal{A}$$

$$\int_{\mathcal{A}_h} \bar{j}\boldsymbol{n}^\alpha(\boldsymbol{\varphi}_h) \cdot \delta\boldsymbol{\varphi}_{,\alpha} d\mathcal{A} + \int_{\mathcal{A}_h} \bar{j}\boldsymbol{l} \cdot \delta\boldsymbol{t}\lambda_h d\mathcal{A} +$$

$$\int_{\mathcal{A}_h} \bar{j}\tilde{\boldsymbol{m}}^\alpha(\boldsymbol{\varphi}_h) \cdot (\delta\boldsymbol{t}\lambda_h)_{,\alpha} d\mathcal{A} + \int_{\partial_I\mathcal{A}_h \cup \partial_T\mathcal{A}_h} [\![\delta\boldsymbol{t} \cdot \bar{j}\lambda_h\tilde{\boldsymbol{m}}^\alpha]\!] \nu_\alpha^- d\partial\mathcal{A} =$$

$$\int_{\partial_N\mathcal{A}_h} \bar{j}\bar{\boldsymbol{n}} \cdot \delta\boldsymbol{\varphi} d\mathcal{A} + \int_{\partial_M\mathcal{A}_h} \bar{j}\bar{\tilde{\boldsymbol{m}}} \cdot \delta\boldsymbol{t}\lambda_h d\mathcal{A} + \int_{\mathcal{A}_h} \boldsymbol{n}^\mathcal{A} \cdot \delta\boldsymbol{\varphi}\bar{j} d\mathcal{A} + \int_{\mathcal{A}_h} \tilde{\boldsymbol{m}}^\mathcal{A} \cdot \delta\boldsymbol{t}\lambda_h\bar{j} d\mathcal{A}$$

Non-linear Shells

- Interface terms rewritten as the sum of 3 terms
  - Introduction of the numerical flux ***h***

$$\int_{\partial_I \mathcal{A}_h} [\![\bar{j}\tilde{\boldsymbol{m}}^{\alpha}(\boldsymbol{\varphi}_h)\cdot\delta\boldsymbol{t}\lambda_h]\!]\,\nu^-_{\alpha}\,d\mathcal{A} \rightarrow \int_{\partial_I \mathcal{A}_h} [\![\delta\boldsymbol{t}]\!]\cdot\boldsymbol{h}\left(\left(\bar{j}\lambda_h\tilde{\boldsymbol{m}}^{\alpha}\right)^+,\,\left(\bar{j}\lambda_h\tilde{\boldsymbol{m}}^{\alpha}\right)^-,\,\nu^-_{\alpha}\right)d\mathcal{A}$$

    - Has to be consistent: $\boldsymbol{h}\left(\lambda_h\bar{j}\tilde{\boldsymbol{m}}^{\alpha}_{\mathrm{exact}},\,\bar{j}\lambda_h\tilde{\boldsymbol{m}}^{\alpha}_{\mathrm{exact}},\,\nu_{\alpha}\right)=\lambda_h\bar{j}\tilde{\boldsymbol{m}}^{\alpha}_{\mathrm{exact}}\nu^-_{\alpha}$
    - One possible choice: $\boldsymbol{h}\left(\left(\bar{j}\lambda_h\tilde{\boldsymbol{m}}^{\alpha}\right)^+,\,\left(\bar{j}\lambda_h\tilde{\boldsymbol{m}}^{\alpha}\right)^-,\,\nu^-_{\alpha}\right)=\nu^-_{\alpha}\left\langle\bar{j}\lambda_h\tilde{\boldsymbol{m}}^{\alpha}\right\rangle$
  - Weak enforcement of the compatibility

$$\int_{\partial_I \mathcal{A}_h} [\![\boldsymbol{t}(\boldsymbol{\varphi}_h)]\!]\cdot\left\langle\delta\left(\bar{j}\lambda_h\tilde{\boldsymbol{m}}^{\alpha}\right)\right\rangle\nu^-_{\alpha}\,d\partial\mathcal{A}$$

Linearization leads to the material tangent modulii $\mathcal{H}_m$

$$\int_{\partial_I \mathcal{A}_h} [\![\boldsymbol{t}(\boldsymbol{\varphi}_h)]\!]\cdot\left\langle\bar{j}_0\mathcal{H}_m^{\alpha\beta\gamma\delta}\left(\delta\boldsymbol{\varphi}_{,\gamma}\cdot\boldsymbol{t}_{,\delta}+\boldsymbol{\varphi}_{,\gamma}\cdot\delta\boldsymbol{t}_{,\delta}\right)\boldsymbol{\varphi}_{,\beta}+\bar{j}\lambda_h\tilde{\boldsymbol{m}}^{\alpha}\cdot\boldsymbol{\varphi}_{,\beta}\;\delta\boldsymbol{\varphi}_{,\beta}\right\rangle\nu^-_{\alpha}\,d\partial\mathcal{A}$$

  - Stabilization controlled by parameter β, for all mesh sizes h^s

$$\int_{\partial_I \mathcal{A}_h \cup \partial_T \mathcal{A}_h} [\![\boldsymbol{t}(\boldsymbol{\varphi}_h)]\!]\cdot\boldsymbol{\varphi}_{,\beta}\left\langle\frac{\beta\bar{j}_0\mathcal{H}_m^{\alpha\beta\gamma\delta}}{h^s}\right\rangle[\![\delta\boldsymbol{t}]\!]\cdot\boldsymbol{\varphi}_{,\gamma}\nu^-_{\alpha}\nu^-_{\delta}\,d\partial\mathcal{A}$$

Non-linear Shells

- New weak formulation

$$\int_{\mathcal{A}_h} \bar{j}\boldsymbol{n}^{\alpha}(\boldsymbol{\varphi}_h)\cdot\delta\boldsymbol{\varphi}_{,\alpha}d\mathcal{A} + \int_{\mathcal{A}_h} \bar{j}\tilde{\boldsymbol{m}}^{\alpha}(\boldsymbol{\varphi}_h)\cdot(\delta\boldsymbol{t}\lambda_h)_{,\alpha}d\mathcal{A} + \int_{\mathcal{A}_h}\bar{j}\boldsymbol{l}\cdot\delta\boldsymbol{t}\lambda_h d\mathcal{A} +$$

$$\int_{\partial_I\mathcal{A}_h\cup\partial_T\mathcal{A}_h} [\![\boldsymbol{t}(\boldsymbol{\varphi}_h)]\!]\cdot\left\langle\bar{j}_0\mathcal{H}_m^{\alpha\beta\gamma\delta}\left(\delta\boldsymbol{\varphi}_{,\gamma}\cdot\boldsymbol{t}_{,\delta}+\boldsymbol{\varphi}_{,\gamma}\cdot\delta\boldsymbol{t}_{,\delta}\right)\boldsymbol{\varphi}_{,\beta}+\bar{j}\lambda_h\tilde{\boldsymbol{m}}^{\alpha}\cdot\boldsymbol{\varphi}_{,\beta}\;\;\delta\boldsymbol{\varphi}_{,\beta}\right\rangle\nu_{\alpha}^{-}d\partial\mathcal{A}$$

$$\int_{\partial_I\mathcal{A}_h\cup\partial_T\mathcal{A}_h}[\![\delta\boldsymbol{t}]\!]\cdot\left\langle\bar{j}\lambda_h\tilde{\boldsymbol{m}}^{\alpha}\right\rangle\nu_{\alpha}^{-}d\partial\mathcal{A} + \int_{\partial_I\mathcal{A}_h\cup\partial_T\mathcal{A}_h}[\![\boldsymbol{t}(\boldsymbol{\varphi}_h)]\!]\cdot\boldsymbol{\varphi}_{,\beta}\left\langle\frac{\beta\bar{j}_0\mathcal{H}_m^{\alpha\beta\gamma\delta}}{h^s}\right\rangle[\![\delta\boldsymbol{t}]\!]\cdot\boldsymbol{\varphi}_{,\gamma}\nu_{\alpha}^{-}\nu_{\delta}^{-}d\partial\mathcal{A} =$$

$$\int_{\partial_N\mathcal{A}_h}\bar{j}\bar{\boldsymbol{n}}\cdot\delta\boldsymbol{\varphi}d\mathcal{A} + \int_{\partial_M\mathcal{A}_h}\bar{j}\bar{\tilde{\boldsymbol{m}}}\cdot\delta\boldsymbol{t}\lambda_h d\mathcal{A} + \int_{\mathcal{A}_h}\boldsymbol{n}^{\mathcal{A}}\cdot\delta\boldsymbol{\varphi}\bar{j}d\mathcal{A} + \int_{\mathcal{A}_h}\tilde{\boldsymbol{m}}^{\mathcal{A}}\cdot\delta\boldsymbol{t}\lambda_h\bar{j}d\mathcal{A}$$

- Implementation
  - Shell elements
    - Membrane and bending responses
    - 2x2 (4x4) Gauss points for bi-quadratic (bi-cubic) quadrangles
  - Interface elements
    - 3 contributions
    - 2 (4) Gauss points for quadratic (cubic) meshes
    - Contributions of neighboring shells evaluated at these points

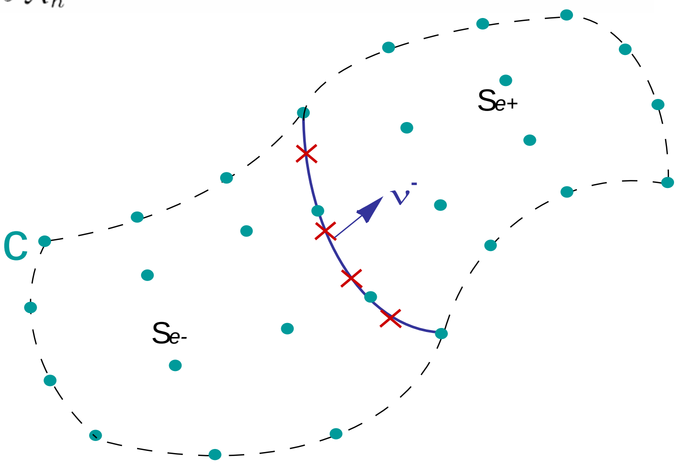

Numerical examples

- Pinched open hemisphere
  - Properties:
    - 18-degree hole
    - Thickness 0.04 m; Radius 10 m
    - Young 68.25 MPa; Poisson 0.3
  - Comparison of the DG methods
    - Quadratic, cubic & distorted el.

    with literature

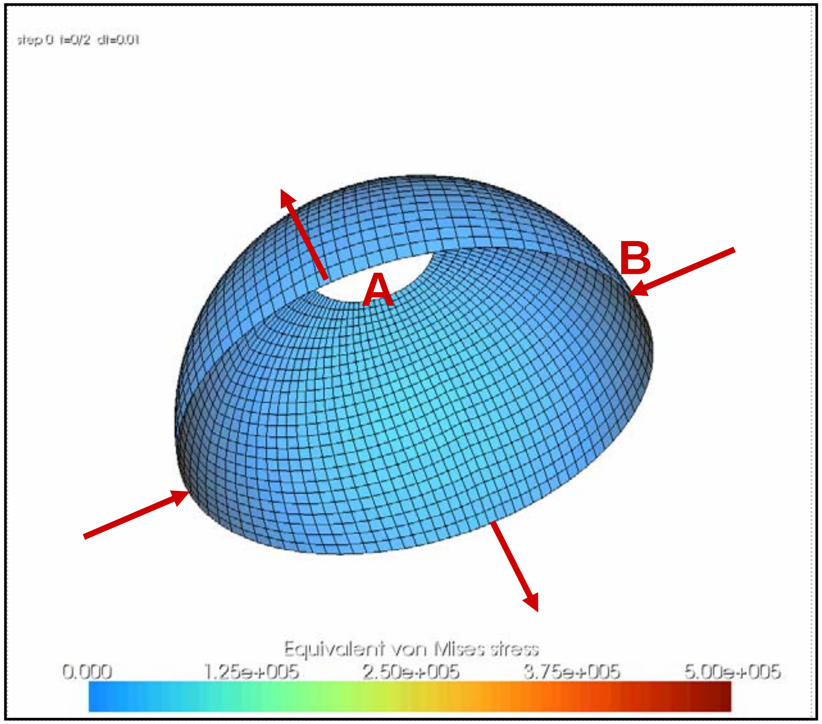

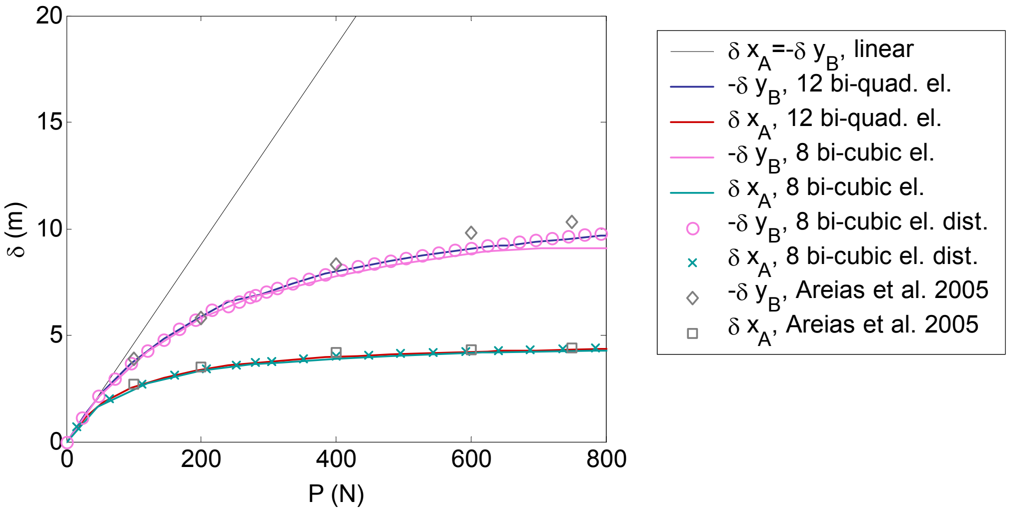

Numerical examples

- Pinched open hemisphere

Influence of the stabilization parameter

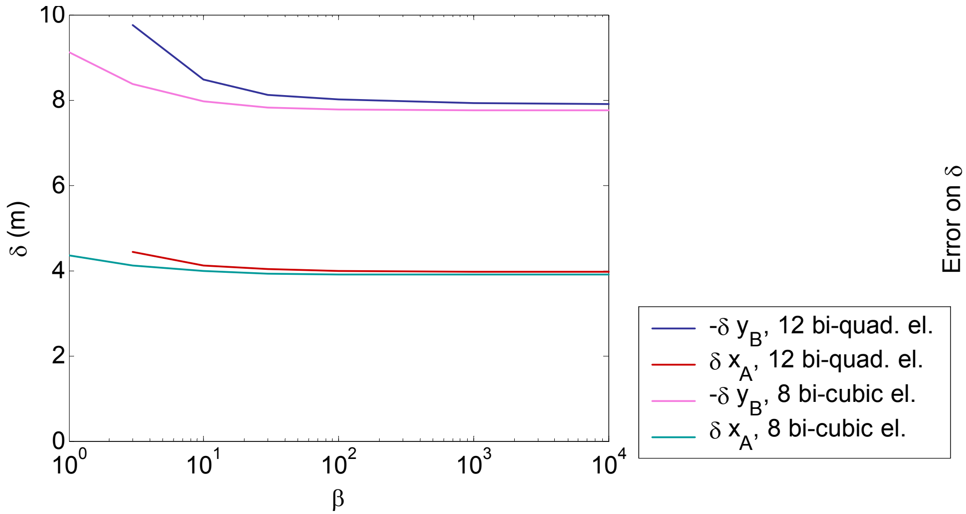

Influence of the mesh size

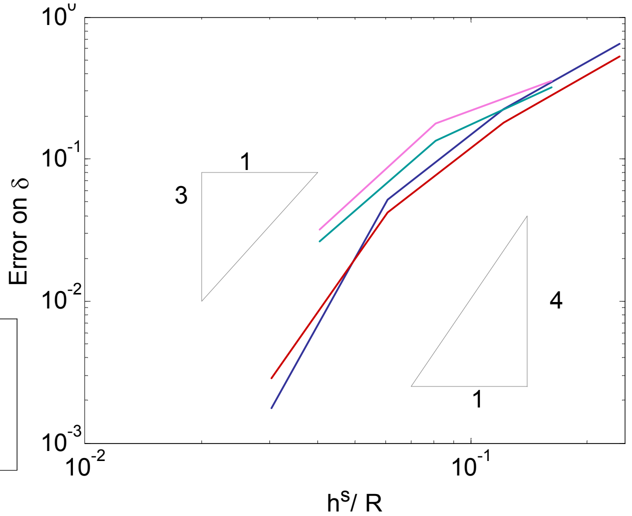

  - Stability if $\beta > 10$
  - Order of convergence in the **L**^{2}-norm in k+1

Numerical examples

- Plate ring
  - Properties:
    - Radii 6 -10 m
    - Thickness 0.03 m
    - Young 12 GPa; Poisson 0
  - Comparison of DG methods
    - Quadratic elements

    with literature

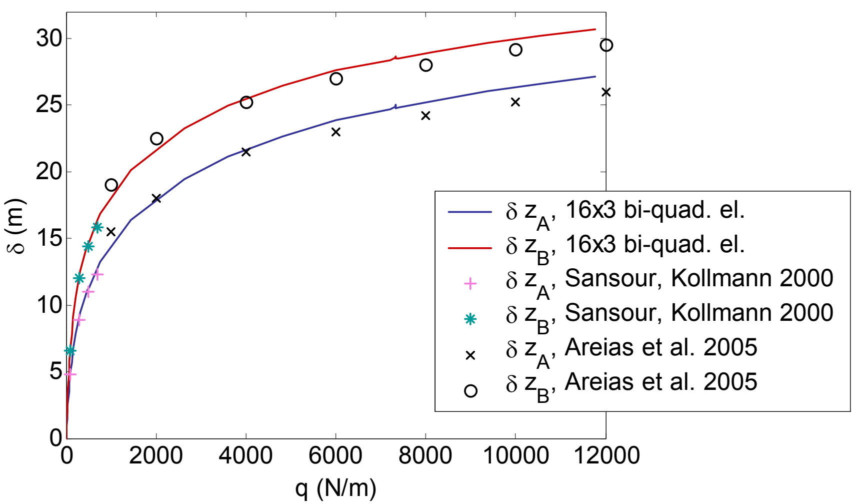

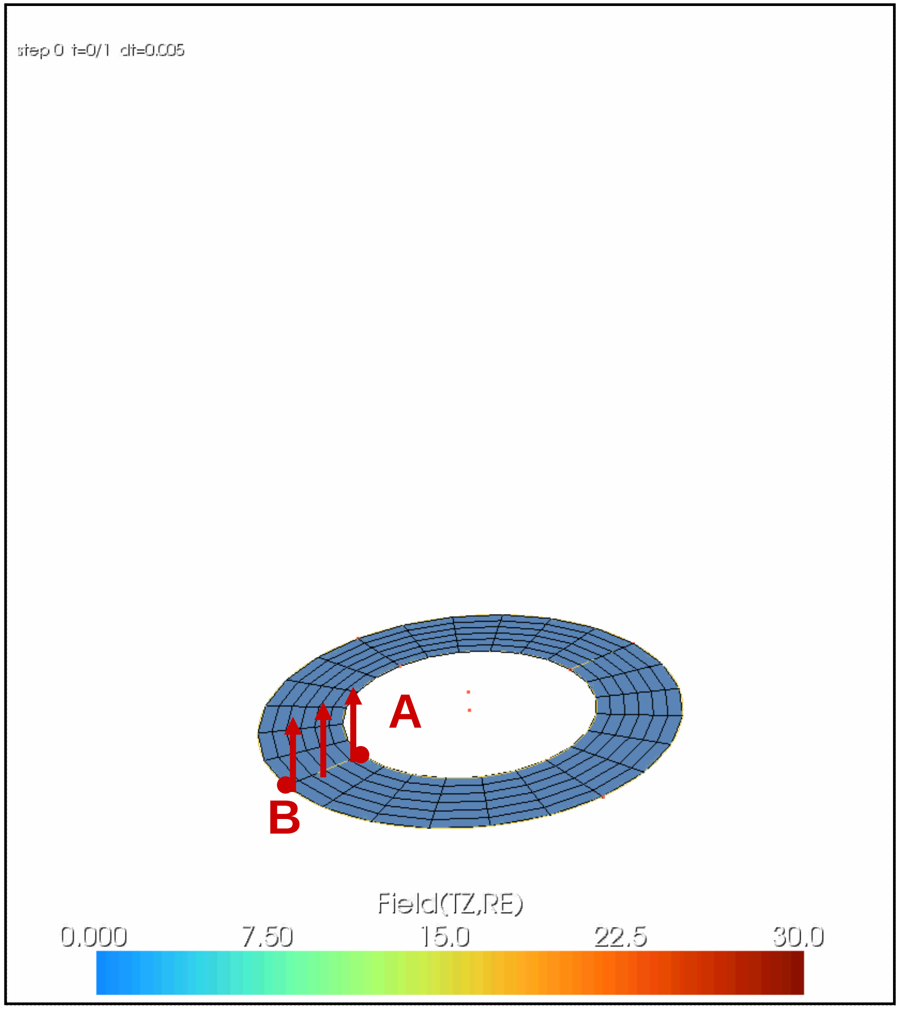

Université de Liège

Numerical examples

- Clamped cylinder
  - Properties:
    - Radius 1.016 m; Length 3.048 m; Thickness 0.03 m
    - Young 20.685 MPa; Poisson 0.3
  - Comparison of DG methods
    - Quadratic & cubic elements

    with literature

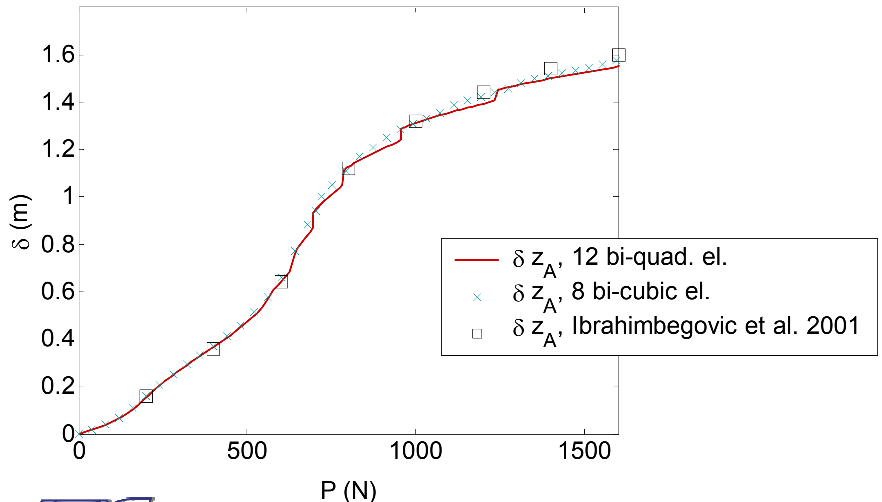

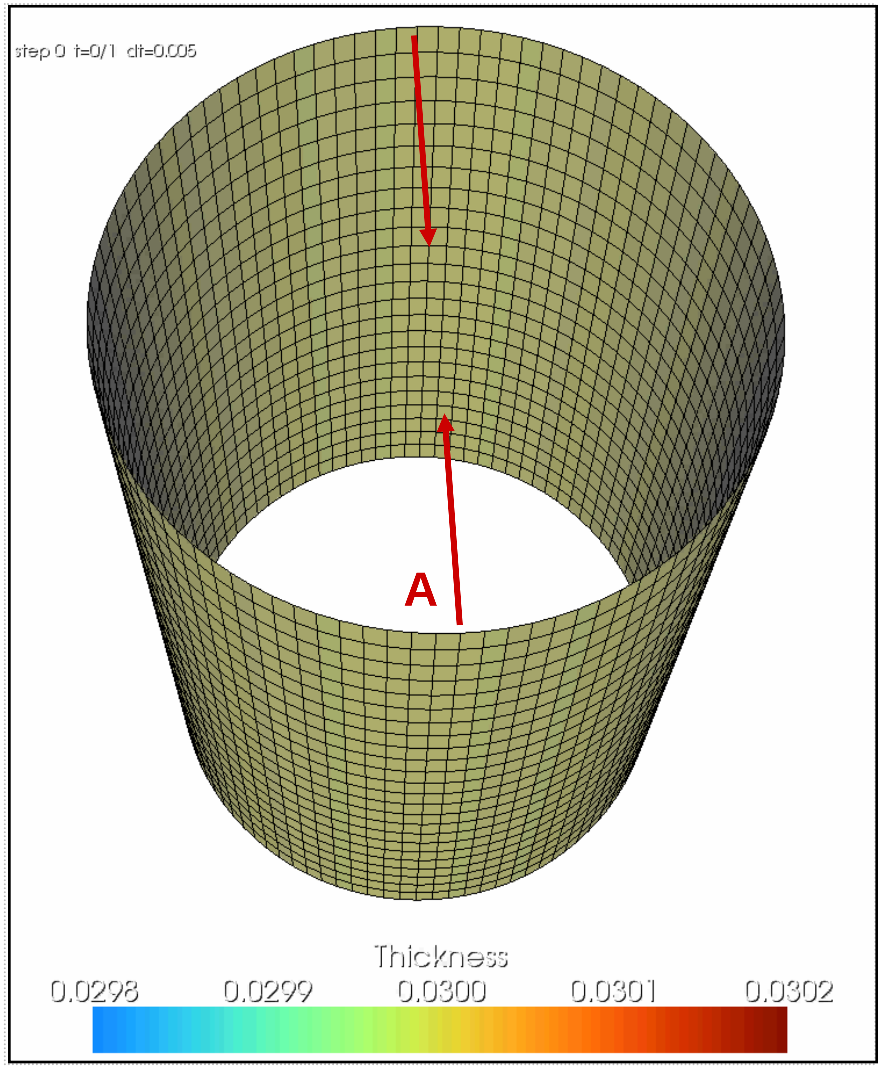

Conclusions & Perspectives

- Development of a discontinuous Galerkin framework for non-linear Kirchhoff-Love shells
  - Displacement formulation (no additional degree of freedom)
    - Strong enforcement of C^0 continuity
    - Weak enforcement of C^1 continuity
  - Quadratic elements:
    - Method is stable if $\beta \geq 10$
    - Reduced integration (but hourglass-free)
  - Cubic elements:
    - Method is stable if $\beta \geq 10$
    - Full Gauss integration (but locking-free)
  - Convergence rate:
    - k-1 in the energy norm
    - k+1 in the L2-norm

Conclusions & Perspectives

- Perspectives
  - Next developments:
    - Plasticity
    - Dynamics …
  - Full DG formulation
    - Displacements and their derivatives discontinuous
    - Application to fracture
  - Application of this displacement formulation to computational homogenization of thin structures